Rapid structural analysis of minute quantities of organic solids by exhausting ^{1}H polarization in solid-state NMR spectroscopy at fast MAS

Zhiwei Yan,[1] Rongchun Zhang[1,2]*

[1]South China Advanced Institute for Soft Matter Science and Technology (AISMST), School of Molecular Science and Engineering (MoSE), South China University of Technology, Guangzhou, 510640, P. R. China

[2]Guangdong Provincial Key Laboratory of Functional and Intelligent Hybrid Materials and Devices, South China University of Technology, Guangzhou, 510640, P. R. China

Corresponding Author

Rongchun Zhang, E-mail: zhangcr@scut.edu.cn

Abstract

Solid-state nuclear magnetic resonance (NMR) is a powerful and indispensable tool for structural and dynamic studies of various challenging systems. Nevertheless, it often suffers from significant limitations due to the inherent low signal sensitivity when low-γ nuclei are involved. Herein, we report an efficient solid-state NMR approach for rapid and efficient structural analysis of minute amounts of organic solids. By encoding staggered chemical shift evolution in the indirect dimension and staggered acquisition in ^{1}H dimension, a proton-detected homonuclear ^{1}H/^{1}H and heteronuclear ^{13}C/^{1}H chemical shift correlation (HETCOR) spectrum can be obtained simultaneously in a single experiment at fast magic-angle-spinning (MAS) conditions with barely increasing experimental time, compared to conventional proton-detected HETCOR experiment. We establish that abundant ^{1}H polarization can be efficiently manipulated and fully utilized in proton-detected solid-state NMR spectroscopy for extraction of more critical structural information and thus reduction of total experimental time.

Via selective manipulation of the spin interactions among nuclei, solid-state nuclear magnetic resonance (NMR) spectroscopy is able to reveal the structural information at a length scale from 0.1nm to about 100nm and dynamic information at a time scale from about 1ps to about 100s in solids.[1] Therefore, solid-state NMR has been playing a significant and indispensable role in providing atomic-level insights into the structures and dynamics of a wide variety of challenging systems over the past few decades, including polymers,[2-3] proteins,[4] drug delivery,[5] and so on. Nevertheless, the inherent low sensitivity of solid-state NMR has severely limited the application range of this mighty technique due to the failure of utilizing the great benefits of sophisticated multidimensional solid-state NMR experiments. In addition, the isotope labelling on organic solids is usually unpractical and prohibitive due to the complicated synthesis protocols and forbidding cost. While the emerging low temperature dynamic nuclear polarization (DNP)[6-8] in recent years can boost the signal sensitivity by more than two orders of magnitude, there are other severe issues with low spectral resolution, probably frozen molecular dynamics at low temperature, structural perturbation due to the incorporation of polarizing agent, and expense in carrying out the experiments. Instead, there is considerable interest in developing proton-based solid-state NMR spectroscopy that fully utilizes the high sensitivity of protons afforded by its highest gyromagnetic ratio and nearly 100% natural abundance.[9-14] Fortunately, in virtue of the tremendous advances in magic-angle-spinning (MAS) probe technologies, spinning can be up to 170 kHz now using a small rotor with a diameter less than 0.5mm,[15-16] and the probe with the capability of spinning beyond 60 kHz has indeed become common in many NMR laboratories. Under

such fast MAS conditions, the strong proton-proton dipolar couplings can be significantly averaged,[17] leading to dramatic enhancement of proton spectral resolution particularly when combined with ultrahigh magnetic field.[17-21] Indeed, we have previously fully exploited multidimensional single channel proton solid-state NMR experiments at fast MAS conditions in order to fully explore the benefits of high sensitivity of protons for structural analysis of minute amounts of organic solids.[22-26] Particularly, homonuclear $^{1}H/^{1}H$ single-quantum/single-quantum (SQ/SQ) and double-quantum/single-quantum (DQ/SQ) correlation experiments are widely adapted for probing the proximity of protons, enabling revealing the hydrogen bonding interactions, intermolecular compatibility and chain packings.[27-29] Nevertheless, it should be noted that the spectral resolution of proton is not comparable to that of ^{13}C spectra, and proton-detected $^{13}C/^{1}H$ heteronuclear correlation (HETCOR) experiment is typically required for accurate proton resonance assignments and thus enabling rapid structural analysis.[30-32] Notably, in the conventional proton-detected HETCOR experiment (Figure 1a),[30, 33] only around 1% of ^{1}H polarization is transferred to ^{13}C via the first cross polarization (CP) period for the natural abundance organic solids, while 99% of ^{1}H polarization is actually destroyed and wasted by the heteronuclear decoupling or HORROR (homonuclear rotary resonance) period[34] to fully eliminate the residual proton polarization before second CP transfer for proton detection. In the previous study, we have well demonstrated that those residual 99% ^{1}H polarization can be further utilized for subsequent multiple CP polarization transfer at fast MAS conditions if the proton $T_{1\rho}$ is long enough, even enabling the direct acquisition of natural abundant ^{13}C NMR spectra using only ~2mg compounds.[35] Indeed, numerous approaches

have been proposed to enhance the sensitivity of solid-state NMR spectroscopy per unit time, enabling extraction of rich structural/dynamic information in a single experiment. On one hand, the experimental time of multidimensional solid-state NMR experiments can be substantially reduced by accelerating ^{1}H spin-lattice relaxation (T_1) time, via recycling residual ^{1}H polarization after low-γ nuclei signal acquisition,[36-38] or selective excitation to accelerate the re-polarization of ^{1}H that are correlated to the heteronuclear spins of interest.[39-40] On the other hand, multiple acquisition can be implemented in a single scan via multiple detector/receivers[41-43] or pulse sequence development by utilizing different magnetization reservoirs and creating multiple polarization transfer pathways. [44-47] Such strategy is also named as parallel NMR spectroscopy, [48-49] which enables obtaining multiple multidimensional solid-state NMR spectra in a single experiment. Notably, due to the typically long T_1 relaxation time, ^{13}C or ^{15}N reservoirs are typically manipulated in parallel to obtain multiple 2D data set from a single experiment.[50] Nevertheless, the tailored manipulation of ^{1}H polarization for parallel acquisitions in a single scan is more challenging and actually less reported.[35, 51-52] Herein, we propose using a combination of staggered chemical shift evolution in indirect dimension and staggered signal acquisition in direct proton dimension, a homonuclear $^{1}H/^{1}H$ correlation, either single-quantum/single-quantum (SQ/SQ) (Figure 1b) or double-quantum/single-quantum (DQ/SQ) (Figure 1c), and a heteronuclear $^{1}H/^{13}C$ chemical shift correlation (HETCOR) spectrum can be obtained simultaneously in a single experiment. Compared to conventional ^{1}H-detected HETCOR experiment at fast MAS conditions, such experiment barely increases the experimental time, and most importantly does not satisfice the signal

sensitivity. We envisage such method can be an efficient approach for rapid resonance assignments and structural analysis of minute amounts of organic solids.

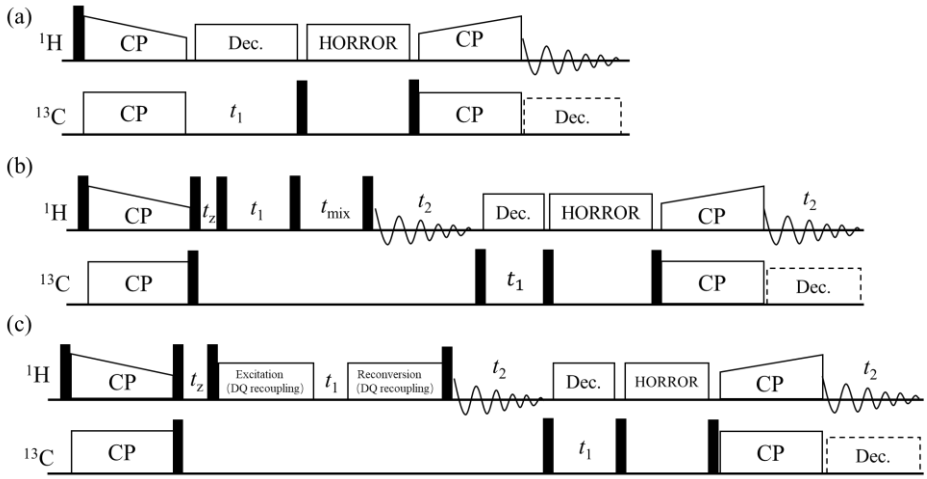

Figure 1. Experimental pulse sequences for (a) conventional 2D ^{1}H-detected HETCOR experiment, (b) 2D ^{1}H-detected SQ-SQ-HETCOR and (c) 2D ^{1}H-detected DQ-SQ-HETCOR experiment. The solid black rectangle indicates the 90^o pulse. Note in both SQ-SQ-HETCOR and DQ-SQ-HETCOR experiments, the two t_1 periods are simultaneously evolved just like a regular 2D experiment.

Our proposed new sequences, denoted as SQ-SQ-HETCOR and DQ-SQ-HETCOR, are shown in Figure 1b and 1c, respectively. In the SQ-SQ-HETCOR experiment, after the first CP period, the ^{1}H and ^{13}C magnetizations are both flipped back to +z direction for storage, and the residual transverse polarization are quickly dephased by the strong proton dipolar couplings during the z-filter time, t_z (~ 1ms). Subsequently, the ^{1}H polarization is flipped to *xy* plane for chemical shift evolution (^{1}H t_1 period), after which ^{1}H polarization is flipped back to +z direction again, and the spin diffusion will occur during the mixing time (t_{mix}) to establish proton SQ/SQ chemical shift correlations. Certainly, homonuclear recoupling sequences,[53] such as finite-pulse radiofrequency driven dipolar recoupling (fp-RFDR),[54-55] amplitude-modulated mixed rotational and rotary-resonance (AM-MIRROR),[56] *etc*., can be incorporated into t_{mix} period to accelerate spin diffusion process.

Finally, a 90° pulse is applied to record the proton signals. After the first proton signal acquisition period, the ^{13}C magnetization is flipped to *xy* plane for chemical shift evolution (^{13}C t_1 period), after which ^{13}C polarization is flipped back to +*z* direction for storage. Subsequently, a short HORROR[34] period (~1ms) is implemented on ^{1}H channel to remove all residual proton magnetization. Finally, the ^{13}C polarization is transferred to proton for detection via second CP polarization transfer period. Similarly, for the DQ-SQ-HETCOR experiment shown in Figure 1c, a DQ recoupling sequence is applied on proton channel after the z-filter to excite DQ coherences. $R18_4^7$ pulse sequence is strongly recommended due to its high DQ recoupling efficiency and superior performance of suppressing t_1-noise induced by MAS fluctuations. [57] After proton DQ chemical shift evolution period, the DQ coherences are converted to zero-quantum (ZQ) coherence by the same DQ recoupling sequence, and then to single-quantum (SQ) coherence by the 90° read pulse for proton detection. After the first proton signal acquisition period, the pulse sequence is just the same as that used in SQ-SQ-HETCOR experiment. It is worth noting that in both SQ-SQ-HETCOR and DQ-SQ-HETCOR experiment, the t_1 evolution period on ^{1}H and ^{13}C channels are simultaneously changed in the experiment just like a regular 2D experiment. Nevertheless, the ^{1}H and ^{13}C t_1 evolution only affects the proton signals in the first and second acquisition period, respectively, in each transient scan. As a result, via the 2D Fourier transformation (FT) with respect to the ^{1}H t_1 evolution and first signal acquisition period, a homonuclear ^{1}H SQ/SQ (or DQ/SQ) spectrum can be obtained, while a heteronuclear $^{13}C/^{1}H$ HETCOR spectrum can be obtained through the 2D FT with respect to the ^{13}C t_1 evolution and second signal acquisition period.

The robust performance of SQ-SQ-HETCOR and DQ-SQ-HETCOR experiments were firstly demonstrated using poly(N-isopropylacrylamide) (PNIPAm) as the model system (Figure 2). From SQ-SQ-HETCOR experiment, both $^{1}H/^{1}H$ SQ/SQ correlation (Figure 2a) and $^{1}H/^{13}C$ HETCOR spectra (Figure 2b) are obtained simultaneously, while the 2D $^{1}H/^{1}H$ DQ/SQ correlation (Figure 2c) and $^{1}H/^{13}C$ HETCOR spectra (Figure 2d) are obtained simultaneously from the single DQ-SQ-HETCOR experiment. For both SQ-SQ-HETCOR and DQ-SQ-HETCOR experiments, the proton chemical shift evolution in the indirect dimension and the first acquisition period will only take a few milliseconds, while the ^{13}C spin-lattice relaxation time (i.e. T_1) is typically several seconds or even tens of seconds. Thus, the ^{13}C magnetization, which is stored along +z direction after the first CP process, will not be affected by the evolution of proton magnetizations during the storage period. Moreover, the experimental time barely increases compared to the conventional proton-detected HETCOR experiment (Figure 1a). As a result, the 2D $^{1}H/^{13}C$ HETCOR spectra obtained from SQ-SQ-HETCOR and DQ-SQ-HETCOR experiment are basically the same (Figure 2b and 2d). Notably, from Figure 2a, a total correlation among protons can be observed due to the efficient proton spin diffusion in a mixing time of 10ms. In addition, we observe an auto-correlation peak at about δ_{SQ}=3ppm in 2D ^{1}H SQ/SQ correlation spectrum (indicated by blue dash line in Figure 2a), which is ascribed to the main chain -CH (H5) proton signal. Nevertheless, it is significantly overlapped with side chain -CH (H3) proton signal, and thus it is not easy to identify H5 signal in the simple 1D proton spectrum (as shown on top of Figure 2a). Besides, since H5 and H6 are close to each other, the DQ correlation between H5 and H6 is quite expected as shown in Figure 2c (indicated by the

red line). Moreover, we can observe that the proton signal at 3ppm is correlated with all the carbon signals in the HETCOR spectra (Figure 2b and 2d) within 1ms CP contact time. Notably, in 2D ^{1}H DQ/SQ correlation spectrum, we do not observe the DQ correlation between -NH protons, implying the absence of intrachain or interchain hydrogen bonding interactions in current sample, and thus the $^{1}H/^{13}C$ correlation between -CO (C4) carbon and -NH proton in 2D $^{1}H/^{13}C$ HETCOR spectrum (Figure 2b and 2d) is mainly coming from the intrachain correlation due to chemical bonding between -CO and -NH groups, instead of interchain hydrogen bonding interactions. Besides, a total $^{1}H/^{13}C$ correlation is also observed in HETCOR spectra since a contact time of 1ms is used for the second CP process, leading to efficient spin diffusion. Certainly, there will be only bonded $^{1}H/^{13}C$ correlation in the HETCOR spectrum if the contact time of the second CP is short enough, such as 0.4ms. Overall, a combination of homonuclear $^{1}H/^{1}H$ and heteronuclear $^{13}C/^{1}H$ correlation spectrum, as obtained from a single experiment, can enable rapid structural analysis and extraction of critical structural information, such as revealing the intrachain or interchain hydrogen bonding interactions.

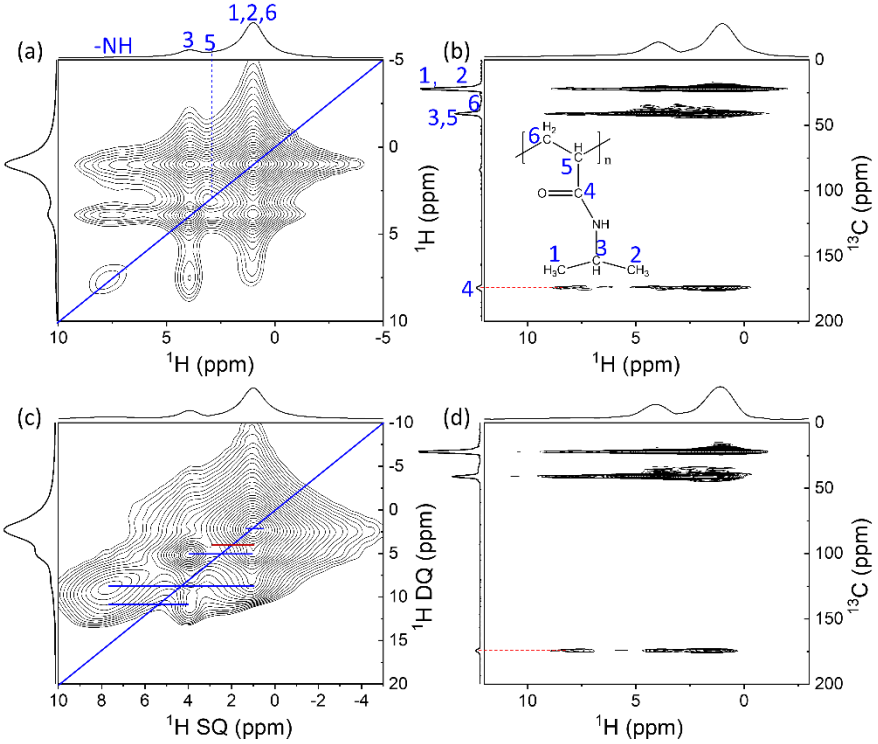

Figure 2. The 2D ^{1}H/^{1}H homonuclear and ^{1}H/^{13}C heteronuclear correlation spectra of poly(N-isopropylacrylamide) (PNIPAm) obtained from SQ-SQ-HETCOR (a, b) and DQ-SQ-HETCOR (c, d) experiment. The schematic molecular structure of PNIPAm was shown as inset in Figure 2b. The blue dash line indicates the main chain -CH proton signal, while the red dash line indicates the correlation between -NH proton and carbonyl carbon. The red solid line indicates the DQ correlation between the main chain -CH proton and the protons at 1.0ppm.

The robust performance of SQ-SQ-HETCOR and DQ-SQ-HETCOR experiments are further examined on the polyacrylic acid (PAA) sample, where the results are shown in Figure 3(a, b) and Figure 3(c, d), respectively. In the proton spectrum, signals at 13.0ppm and 7.9ppm are ascribed to hydrogen-bonded cyclic dimers of -COOH and nonhydrogen-bonded -COOH protons, respectively. [58-60] This is well confirmed by the 2D ^{1}H DQ/SQ spectrum shown in Figure 3c, where an auto-correlation DQ signal at (δ_{DQ}=26ppm, δ_{SQ}=13.0ppm) is clearly observed, while the auto-correlation DQ signal of the nonhydrogen-bonded carbonyl proton (δ_{SQ}=7.9ppm) is not observed due to the absence of hydrogen bonding interactions. In addition, we also observed an auto-

correlation DQ signal at (δ_{DQ}=21.8ppm, δ_{SQ}=10.9ppm). Indeed, the proton signal at 10.9 ppm is typically ascribed to exchange of hydrogen-bonded and free -COOH protons.[59] Besides, from the 2D DQ/SQ spectrum, we do not observed the DQ correlation between the proton signal at 10.9ppm and that at 13.0ppm, which may be due to the fast dynamic exchange process between the hydrogen-bonded dimer and the free -COOH form.[59] The ^{1}H resonance assignments can be further supported by the 2D ^{1}H/^{13}C HETCOR spectra (Figure 3b and 3d). Two different ^{13}C chemical shift values of carbonyl groups are observed, where the ^{13}C peak at 178.4ppm and 182.5ppm is ascribed to the free and hydrogen-bonded carbonyl group, respectively. As a result, the proton signal at 13.0ppm only correlates with the carbon signal at 182.5ppm due to the hydrogen bonding interactions between the cyclic dimers of -COOH group, while the free -COOH group is indicated by the correlation at (δ_{13C}=178.4ppm, δ_{1H}=7.9ppm) due to absence of hydrogen bonds. Note that the proton signal at 10.9ppm is correlated with the carbon signal at 178.4ppm (indicated by the red dash lines in Figure 3b), implying that the protons are mostly in the free -COOH state instead of dimers despite of the exchange process between hydrogen-bonded dimers and free -COOH forms.

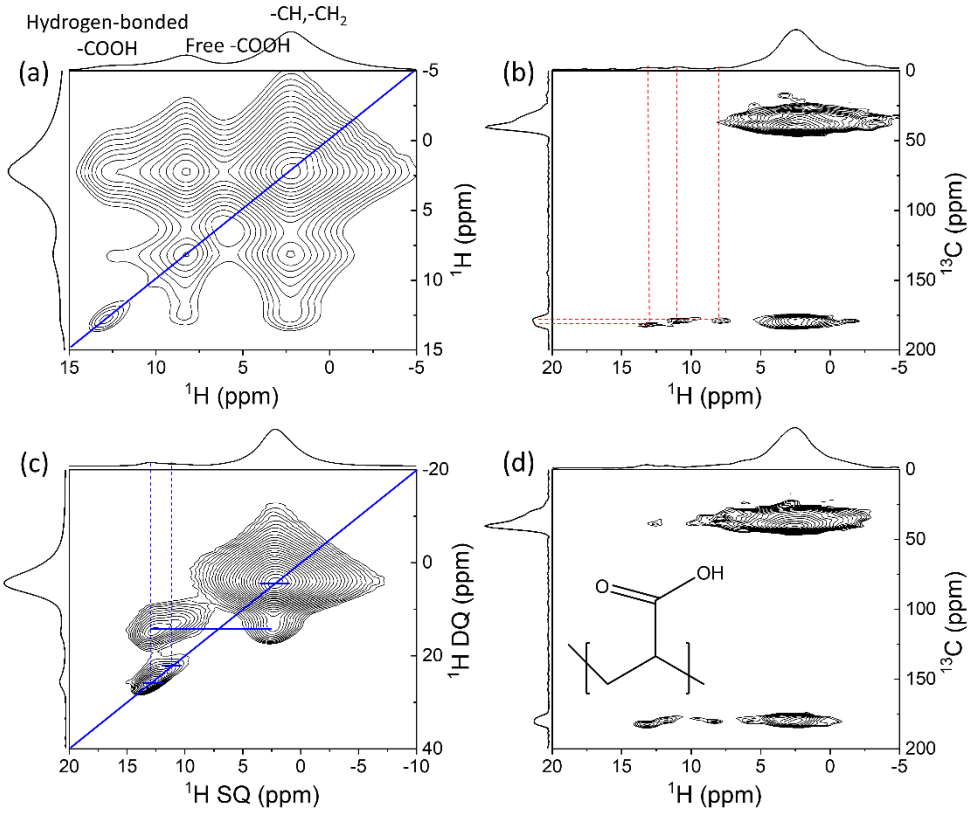

Figure 3. The 2D $^{1}H/^{1}H$ homonuclear and $^{1}H/^{13}C$ heteronuclear correlation spectra of polyacrylic acid (PNIPAm) obtained from SQ-SQ-HETCOR (a, b) and DQ-SQ-HETCOR (c, d) experiment. The schematic molecular structure of PAA was shown as inset. The blue dash lines indicate the proton signals at 13.0ppm and 10.9ppm, corresponding to the hydrogen-bonded cyclic dimers of -COOH, and the exchange of hydrogen-bonded and free -COOH protons, respectively. The red dash lines indicate the $^{1}H/^{13}C$ correlations among carbonyl groups.

It is worth emphasizing that for both SQ-SQ-HETCOR and DQ-SQ-HETCOR experiments, the indirect ^{1}H and ^{13}C chemical shift evolution periods are simultaneously changed as the regular 2D chemical shift correlation experiments. It means the spectral width and chemical shift evolution time in the indirect ^{1}H and ^{13}C dimensions are exactly the same. However, the ^{1}H and ^{13}C chemical shift evolution in the indirect dimension has independent influence on the acquired proton signals in the first and second acquisition periods, respectively. That's why we can simultaneously and independently obtain a homonuclear and heteronuclear chemical shift correlation spectrum from a single

experiment via simple 2D FT. Also, for both SQ-SQ-HETCOR and DQ-SQ-HETCOR experiments, a short HORROR period around 1ms is typically required before the second CP process. This guarantees that acquired proton signals in the second acquisition period is purely coming from the second $^{13}C \rightarrow {}^{1}H$ CP process instead of residual proton magnetization. In fact, without the use of HORROR period, there will be significant t_1-noise in the obtained 2D spectra, leading to substantial compromise of the signal-to-noise ratio of 2D spectra.

In summary, the abundant ^{1}H polarization in conventional proton-detected HETCOR experiment can be further exhausted, via innovative pulse sequence design, to obtain another homonuclear $^{1}H/^{1}H$ SQ/SQ or DQ/SQ correlation spectrum at fast MAS conditions. This is indeed achieved by creatively encoding staggered chemical shift evolution in the indirect ^{1}H and ^{13}C dimension and staggered acquisition in the direct ^{1}H dimension, where indirect ^{1}H and ^{13}C chemical shift evolution has independent and separated influence on the acquired proton signals in the first and second acquisition period, respectively. As a result, both homonuclear $^{1}H/^{1}H$ and heteronuclear $^{1}H/^{13}C$ correlation spectra can be simultaneously obtained from a single experiment. Moreover, the experimental time increases little compared to conventional HETCOR experiment as it only takes ~20ms more in each transient scan. The robust performance of SQ-SQ-HETCOR and DQ-SQ-HETCOR experiments are well demonstrated on PNIPAm and PAA samples, using only ~2mg sample at 60 kHz MAS and 400 MHz magnetic field, and it is anticipated that the use of higher MAS frequency (such as 150 kHz) and stronger magnetic field (such as 1.2 GHz) can further boost the spectral resolution and signal sensitivity. We hope the core

idea in this study, namely exhausting ^{1}H polarization in each transient scan, can inspire the development of new solid-state NMR techniques under fast MAS conditions to enhance the sensitivity of solid-state NMR spectroscopy. We foresee that the reported SQ-SQ-HETCOR and DQ-SQ-HETCOR approaches can be valuable for the study of a broad range of molecular systems, such as zeolites, pharmaceuticals, covalent-organic frameworks (COF), and so on.

Experimental Section

All samples were purchased from Sigma-Aldrich, and used as received without any further purification. All solid-state NMR experiments were performed at 9.4 T on a JEOL JNM-ECZR400R/M1 spectrometer with a 1.0mm HX MAS probe (JEOL RESONANCE Inc., Japan). The magic-angle spinning (MAS) frequency was automatically controlled at 60 kHz. For all the experiments, ^{1}H and ^{13}C 90^{o} pulse length was both set as 1.0 μs. The contact time for the first and second CP was set as 2ms and 1ms, respectively. The RF strength during CP was around 145 kHz and 85 kHz on ^{1}H and ^{13}C channel, respectively, with a 9% ramp on ^{13}C channel. SPINAL64 decoupling[61] scheme was adapted for ^{1}H decoupling during ^{13}C chemical shift evolution with a ^{1}H radiofrequency strength around 15 kHz. The z-filter time after the first CP process was set as 1ms and 4ms for SQ-SQ-HETCOR and DQ-SQ-HETCOR experiment, respectively. A spin diffusion mixing time of 10ms was used for the SQ-SQ-HETCOR experiment. The indirect spectral width was set as 30 kHz for all experiments. $R18_4^7$ sequence[57] was adapted to excite DQ coherence with a total

recoupling time of 4 rotor periods, and the RF field strength was set the same as the theoretical RF strength, *i.e.* 2.25ν_r., where ν_r is the MAS frequency. The recycle delay was set as 1s and 2s for the experiments on PAA and PNIPAm, respectively. States-TPPI[62]method was employed for the quadrature detection along the indirect dimension with 64 and 128 t_1 increments for experiments on PAA and PNIPAm, respectively.

ASSOCIATED CONTENT

AUTHOR INFORMATION

Corresponding Author

*E-mail: zhangcr@scut.edu.cn (R. Zhang)

ORCID

Rongchun Zhang: 0000-0002-2480-2652

Zhiwei Yan: 0000-0002-0727-6048

Notes

The authors declare no competing financial interests.

ACKNOWLEDGMENT

The authors acknowledge the financial supports by the National Natural Science Foundation of China (No. 21973031), Natural Science Foundation of Guangdong Province, China (No. 2019A1515011140 and 2016ZT06C322), and the R&D program of Guangzhou, China (No. 202102020941).

REFERENCES

1. Mehring, M. *Principles of high resolution NMR in solids*. Springer-Verlag Berlin Heidellberg, copyright, 1983.
2. Zhang, R.; Miyoshi, T.; Sun, P., Eds. *NMR Methods for Characterization of Synthetic and Natural Polymers.* Royal Society of Chemistry, Copyright 2019.
3. Schmidt-Rohr, K.; Spiess, H. W. *Multidimensional solid-state NMR and polymers*. Academic Press: London, 1994.
4. Separovic, F.; Naito, A. *Advances in biological solid-state NMR: proteins and membrane-active peptides*. Royal Society of Chemistry, Copyright 2014.
5. Marchetti, A.; Yin, J.; Su, Y.; Kong, X. Solid-state NMR in the field of drug delivery: State of the art and new perspectives. *Magn. Reson. Lett.* 2021, 1(1), 28-70.
6. Tycko, R. NMR at Low and Ultralow Temperatures. *Acc. Chem. Res*., 2013, 46 (9), 1923-1932.
7. Rossini, A. J.; Zagdoun, A.; Lelli, M.; Lesage, A.; Copéret, C.; Emsley, L. Dynamic Nuclear Polarization Surface Enhanced NMR Spectroscopy. *Acc. Chem. Res.,* 2013, 46 (9), 1942-1951.
8. Maly, T.; Debelouchina, G. T.; Bajaj, V. S.; Hu, K.-N.; Joo, C.-G.; Mak–Jurkauskas, M. L.; Sirigiri, J. R.; Wel, P. C. A. v. d.; Herzfeld, J.; Temkin, R. J.; Griffin, R. G. Dynamic nuclear polarization at high magnetic fields. *J. Chem. Phys.,* 2008, 128 (5), 052211.
9. Zhang, R.; Mroue, K. H.; Ramamoorthy, A. Proton-Based Ultrafast Magic Angle Spinning Solid-State NMR Spectroscopy. *Acc. Chem. Res.,* 2017, 50 (4), 1105-1113.
10. Nishiyama, Y. Fast magic-angle sample spinning solid-state NMR at 60–100 kHz for natural abundance samples. *Solid State Nucl. Magn. Reson.* 2016, 78, 24-36.
11. Vasa, S. K.; Rovó, P.; Linser, R. Protons as Versatile Reporters in Solid-State NMR Spectroscopy. *Acc. Chem. Res.* 2018, 51 (6), 1386-1395.
12. Ishii, Y.; Wickramasinghe, A.; Matsuda, I.; Endo, Y.; Ishii, Y.; Nishiyama, Y.; Nemoto, T.; Kamihara, T. Progress in proton-detected solid-state NMR (SSNMR): Super-fast 2D SSNMR collection for nano-mole-scale proteins. *J. Magn. Reson.* 2018, 286, 99-109.
13. Duong, N. T.; Raran-Kurussi, S.; Nishiyama, Y.; Agarwal, V. Quantitative 1H–1H Distances in Protonated Solids by Frequency-Selective Recoupling at Fast Magic Angle Spinning NMR. *J. Phys. Chem. Lett.* 2018, 9 (20), 5948-5954.
14. Zhang, Z.; Oss, A.; Org, M.-L.; Samoson, A.; Li, M.; Tan, H.; Su, Y.; Yang, J. Selectively enhanced 1H–1H correlations in proton-detected solid-state NMR under ultrafast MAS conditions. *J. Phys. Chem. Lett.,* 2020, 11 (19), 8077-8083.
15. Samoson, A. H-MAS. *J. Magn. Reson.,* 2019, 306, 167-172.
16. Lin, Y.-L.; Cheng, Y.-S.; Ho, C.-I.; Guo, Z.-H.; Huang, S.-J.; Org, M.-L.; Oss, A.; Samoson, A.; Chan, J. C. C. Preparation of fibril nuclei of beta-amyloid peptides in reverse micelles. *Chem. Commun.,* 2018, 54 (74), 10459-10462.
17. Böckmann, A.; Ernst, M.; Meier, B. H. Spinning proteins, the faster, the better? *J. Magn. Reson.* 2015, 253, 71-79.
18. Pandey, M. K.; Zhang, R.; Hashi, K.; Ohki, S.; Nishijima, G.; Matsumoto, S.; Noguchi, T.; Deguchi, K.; Goto, A.; Shimizu, T.; Maeda, H.; Takahashi, M.; Yanagisawa, Y.; Yamazaki, T.; Iguchi, S.; Tanaka, R.; Nemoto, T.; Miyamoto, T.; Suematsu, H.; Saito, K.; Miki, T.; Ramamoorthy, A.; Nishiyama, Y. 1020 MHz single-channel proton fast magic angle spinning solid-state NMR spectroscopy. *J. Magn. Reson.,* 2015, 261, 1-5.
19. Xue, K.; Sarkar, R.; Lalli, D.; Koch, B.; Pintacuda, G.; Tosner, Z.; Reif, B. Impact of Magnetic

Field Strength on Resolution and Sensitivity of Proton Resonances in Biological Solids. *J. Phys. Chem. C,* 2020, 124 (41), 22631-22637.

20. Nimerovsky, E.; Movellan, K. T.; Zhang, X. C.; Forster, M. C.; Najbauer, E.; Xue, K.; Dervişoğlu, R.; Giller, K.; Griesinger, C.; Becker, S.; Andreas, L. B. Proton Detected Solid-State NMR of Membrane Proteins at 28 Tesla (1.2 GHz) and 100 kHz Magic-Angle Spinning. *Biomolecules* 2021, 11 (5), 752.

21. Callon, M.; Malär, A. A.; Pfister, S.; Římal, V.; Weber, M. E.; Wiegand, T.; Zehnder, J.; Chávez, M.; Cadalbert, R.; Deb, R.; Däpp, A.; Fogeron, M.-L.; Hunkeler, A.; Lecoq, L.; Torosyan, A.; Zyla, D.; Glockshuber, R.; Jonas, S.; Nassal, M.; Ernst, M.; Böckmann, A.; Meier, B. H. Biomolecular solid-state NMR spectroscopy at 1200 MHz: the gain in resolution. *J. Biomol. NMR* 2021, 75 (6), 255-272.

22. Zhang, R.; Pandey, M. K.; Nishiyama, Y.; Ramamoorthy, A. A Novel High-Resolution and Sensitivity-Enhanced Three-Dimensional Solid-State NMR Experiment Under Ultrafast Magic Angle Spinning Conditions. *Sci. Rep*. 2015, 5, 11810.

23. Zhang, R.; Duong, N. T.; Nishiyama, Y.; Ramamoorthy, A. 3D Double-Quantum/Double-Quantum Exchange Spectroscopy of Protons under 100 kHz Magic Angle Spinning. *J. Phys. Chem. B,* 2017, 121 (24), 5944-5952.

24. Zhang, R.; Duong, N. T.; Nishiyama, Y. Resolution enhancement and proton proximity probed by 3D TQ/DQ/SQ proton NMR spectroscopy under ultrafast magic-angle-spinning beyond 70 kHz. *J. Magn. Reson.* 2019, 304, 78-86.

25. Nishiyama, Y.; Agarwal, V.; Zhang, R. t1-Noise Suppression by γ-Free Recoupling Sequences in Solid-State NMR for Structural Characterization of Fully Protonated Molecules at Fast MAS. *J. Phys. Chem. C* 2020, 124 (48), 26332-26343.

26. Zhang, R.; Mroue, K. H.; Ramamoorthy, A. Proton chemical shift tensors determined by 3D ultrafast MAS double-quantum NMR spectroscopy. *J. Chem. Phys.* 2015, 143 (14), 144201.

27. Hansen, M. R.; Graf, R.; Sekharan, S.; Sebastiani, D. Columnar Packing Motifs of Functionalized Perylene Derivatives: Local Molecular Order Despite Long-Range Disorder. *J. Am. Chem. Soc.* 2009, 131 (14), 5251-5256.

28. Zhang, C.; Yang, Z.; Duong, N. T.; Li, X.; Nishiyama, Y.; Wu, Q.; Zhang, R.; Sun, P. Using Dynamic Bonds to Enhance the Mechanical Performance: From Microscopic Molecular Interactions to Macroscopic Properties. *Macromolecules* 2019, 52 (13), 5014-5025.

29. He, X.; Liu, Y.; Zhang, R.; Wu, Q.; Chen, T.; Sun, P.; Wang, X.; Xue, G. Unique Interphase and Cross-Linked Network Controlled by Different Miscible Blocks in Nanostructured Epoxy/Block Copolymer Blends Characterized by Solid-State NMR. *J. Phys. Chem. C* 2014, 118 (24), 13285-13299.

30. Zhou, D. H.; Rienstra, C. M. Rapid Analysis of Organic Compounds by Proton-Detected Heteronuclear Correlation NMR Spectroscopy with 40 kHz Magic-Angle Spinning. *Angew. Chem*. 2008, 120 (38), 7438-7441.

31. Holland, G. P.; Mou, Q.; Yarger, J. L. Determining hydrogen-bond interactions in spider silk with 1H-13C HETCOR fast MAS solid-state NMR and DFT proton chemical shift calculations. *Chem. Commun.* 2013, 49 (59), 6680-6682.

32. Lu, X.; Xu, W.; Hanada, M.; Jermain, S. V.; Williams, R. O.; Su, Y. Solid-state NMR analysis of crystalline and amorphous Indomethacin: An experimental protocol for full resonance assignments. *J. Pharm. Biomed. Anal.,* 2019, 165, 47-55.

33. Ishii, Y.; Yesinowski, J. P.; Tycko, R. Sensitivity Enhancement in Solid-State 13C NMR of Synthetic Polymers and Biopolymers by 1H NMR Detection with High-Speed Magic Angle Spinning. *J. Am. Chem. Soc.* 2001, 123 (12), 2921-2922.
34. Nielsen, N. C.; Bildso/e, H.; Jakobsen, H. J.; Levitt, M. H. Double-quantum homonuclear rotary resonance: Efficient dipolar recovery in magic-angle spinning nuclear magnetic resonance. *J. Chem. Phys.* 1994, 101 (3), 1805-1812.
35. Zhang, R.; Chen, Y.; Rodriguez-Hornedo, N.; Ramamoorthy, A. Enhancing NMR Sensitivity of Natural-Abundance Low-γ Nuclei by Ultrafast Magic-Angle-Spinning Solid-State NMR Spectroscopy. *ChemPhysChem* 2016, 17 (19), 2962-2966.
36. Ye, Y.-Q.; Martineau-Corcos, C.; Taulelle, F.; Nishiyama, Y. Maximizing the sensitivity in 13C cross-polarization magic-angle-spinning solid-state NMR measurements with flip-back pulses. *J. Magn. Reson.* 2018, 294, 122-127.
37. Duong, N. T.; Yarava, J. R.; Trébosc, J.; Nishiyama, Y.; Amoureux, J.-P. Forcing the 'lazy' protons to work. *Phys. Chem. Chem. Phys.* 2018, 20 (40), 25829-25840.
38. Tegenfeldt, J.; Haeberlen, U. Cross polarization in solids with flip-back of I-spin magnetization. *J. Magn. Reson.,* 1979, 36 (3), 453-457.
39. Wijesekara, A. V.; Venkatesh, A.; Lampkin, B. J.; VanVeller, B.; Lubach, J. W.; Nagapudi, K.; Hung, I.; Gor'kov, P. L.; Gan, Z.; Rossini, A. J. Fast Acquisition of Proton-Detected HETCOR Solid-State NMR Spectra of Quadrupolar Nuclei and Rapid Measurement of NH Bond Lengths by Frequency Selective HMQC and RESPDOR Pulse Sequences. *Chem. Eur. J,* 2020, 26 (35), 7881-7888.
40. Han, R.; Yang, Y.; Wang, S. Longitudinal Relaxation Optimization Enhances 1H-Detected HSQC in Solid-State NMR Spectroscopy on Challenging Biological Systems. *Chem. Eur. J,* 2019, 25 (16), 4115-4122.
41. Gopinath, T.; Weber, D. K.; Veglia, G. Multi-receiver solid-state NMR using polarization optimized experiments (POE) at ultrafast magic angle spinning. *J. Biomol. NMR* 2020, 74 (4), 267-285.
42. Martineau, C.; Decker, F.; Engelke, F.; Taulelle, F. Parallelizing acquisitions of solid-state NMR spectra with multi-channel probe and multi-receivers: Applications to nanoporous solids. *Solid State Nucl. Magn. Reson.* 2013, 55-56, 48-53.
43. Gallo, A.; Franks, W. T.; Lewandowski, J. R. A suite of solid-state NMR experiments to utilize orphaned magnetization for assignment of proteins using parallel high and low gamma detection. *J. Magn. Reson.* 2019, 305, 219-231.
44. Gopinath, T.; Veglia, G. Dual Acquisition Magic-Angle Spinning Solid-State NMR-Spectroscopy: Simultaneous Acquisition of Multidimensional Spectra of Biomacromolecules. *Angew. Chem. Int. Ed.* 2012, 51 (11), 2731-2735.
45. Gopinath, T.; Veglia, G. 3D DUMAS: Simultaneous acquisition of three-dimensional magic angle spinning solid-state NMR experiments of proteins. *J. Magn. Reson.,* 2012, 220 (0), 79-84.
46. Gopinath, T.; Veglia, G. Multiple acquisitions via sequential transfer of orphan spin polarization (MAeSTOSO): how far can we push residual spin polarization in solid-state NMR? *J. Magn. Reson.* 2016, 267, 1-8.
47. Stanek, J.; Schubeis, T.; Paluch, P.; Güntert, P.; Andreas, L. B.; Pintacuda, G. Automated Backbone NMR Resonance Assignment of Large Proteins Using Redundant Linking from a Single Simultaneous Acquisition. *J. Am. Chem. Soc*. 2020, 142 (12), 5793-5799.

48. Kupče, Ē.; Frydman, L.; Webb, A. G.; Yong, J. R. J.; Claridge, T. D. W. Parallel nuclear magnetic resonance spectroscopy. *Nat. Rev. Methods Primers,* 2021, 1 (1), 27.
49. Kupče, Ē.; Mote, K. R.; Webb, A.; Madhu, P. K.; Claridge, T. D. W. Multiplexing experiments in NMR and multi-nuclear MRI. *Prog. Nucl. Magn. Reson. Spectrosc.* 2021, 124-125, 1-56.
50. Gopinath, T.; Veglia, G. Orphan Spin Polarization: A Catalyst for High-Throughput Solid-State NMR Spectroscopy of Proteins. *Annu. Rep. NMR Spectrosc.* 2016, 89, 103-121.
51. Zhang, R.; Mroue, K. H.; Ramamoorthy, A. Hybridizing cross-polarization with NOE or refocused-INEPT enhances the sensitivity of MAS NMR spectroscopy. *J. Magn. Reson.* 2016, 266, 59-66.
52. Zhang, R.; Nishiyama, Y.; Ramamoorthy, A. Exploiting heterogeneous time scale of dynamics to enhance 2D HETCOR solid-state NMR sensitivity. *J. Magn. Reson.* 2019, 309, 106615.
53. Duong, N. T.; Raran-Kurussi, S.; Nishiyama, Y.; Agarwal, V. Can proton-proton recoupling in fully protonated solids provide quantitative, selective and efficient polarization transfer? *J. Magn. Reson.* 2020, 317, 106777.
54. Zhang, R.; Nishiyama, Y.; Sun, P.; Ramamoorthy, A. Phase cycling schemes for finite-pulse-RFDR MAS solid state NMR experiments. *J. Magn. Reson.* 2015, 252, 55-66.
55. Ishii, Y. 13C–13C dipolar recoupling under very fast magic angle spinning in solid-state nuclear magnetic resonance: Applications to distance measurements, spectral assignments, and high-throughput secondary-structure determination. *J. Chem. Phys.* 2001, 114 (19), 8473-8483.
56. Scholz, I.; Huber, M.; Manolikas, T.; Meier, B. H.; Ernst, M. MIRROR recoupling and its application to spin diffusion under fast magic-angle spinning. *Chem. Phys. Lett.* 2008, 460 (1), 278-283.
57. Nishiyama, Y.; Agarwal, V.; Zhang, R. Efficient symmetry-based γ-encoded DQ recoupling sequences for suppression of t1-Noise in solid-state NMR spectroscopy at fast MAS. *Solid State Nucl. Magn. Reson.* 2021, 114, 101734.
58. Li, B.; Xu, L.; Wu, Q.; Chen, T.; Sun, P.; Jin, Q.; Ding, D.; Wang, X.; Xue, G.; Shi, A.-C. Various Types of Hydrogen Bonds, Their Temperature Dependence and Water−Polymer Interaction in Hydrated Poly(Acrylic Acid) as Revealed by 1H Solid-State NMR Spectroscopy. *Macromolecules* 2007, 40 (16), 5776-5786.
59. Akbey, Ü.; Graf, R.; Peng, Y. G.; Chu, P. P.; Spiess, H. W. Solid-State NMR investigations of anhydrous proton-conducting acid–base poly(acrylic acid)– poly(4-vinyl pyridine) polymer blend system: A study of hydrogen bonding and proton conduction. *J. Polym. Sci. Part B: Polym. Phys.* 2009, 47 (2), 138-155.
60. Fenfen Wang, P. W., Hongyao Niu, Yingfeng Yu, Pingchuan Sun. Solid-State NMR Studies on Hydrogen Bonding Interactions and Structural Evolution in PAA/PEO Blends. *Acta Phys. -Chim. Sin.* 2020, 36 (4), 1912016.
61. Fung, B. M.; Khitrin, A. K.; Ermolaev, K. An Improved Broadband Decoupling Sequence for Liquid Crystals and Solids. *J. Magn. Reson.* 2000, 142 (1), 97-101.
62. States, D. J.; Haberkorn, R. A.; Ruben, D. J. A two-dimensional nuclear overhauser experiment with pure absorption phase in four quadrants. *J. Magn. Reson.*1982, 48 (2), 286-292.